EFFECTS OF LOADING FREQUENCY AND ENVIRONMENT ON HIGH TEMPERATURE FATIGUE CRACK GROWTH IN NICKEL-BASE ALLOYS

R. B. Scarlin*

INTRODUCTION

It has been known for several years that the high temperature life of smooth specimens is dependent on the testing frequency and decreases as the testing frequency is reduced [1]. However crack initiation and propagation may be differently affected by changes of frequency, and endurance results do not enable the effect on each to be separately studied. For example, at low frequencies and stress intensities initiation in Udimet 700 at 760°C is at surface grain boundaries and propagation is intergranular. However, at higher frequencies initiation occurs at subsurface brittle phases and propagation is transgranular. In crack propagation tests [2, 3, 4] it has similarly been determined that growth rates per load cycle are increased as the testing frequency is reduced below a critical value and the crack propagation path changes from trans- to intergranular.

The increase in growth rate has been attributed to the interaction with fatigue of time-dependent effects such as creep and oxidation, and becomes more important as the time per cycle is increased. Tests at different frequencies in vacuum should show whether creep or oxidation is of more importance. Recent work on the iron-nickel base superalloy, A286 [5] and cast nickel base Udimet 500 [6], at frequencies down to 3 x 10^{-3}Hz, has indicated that the low frequency crack acceleration in these cases may be due to environmental effects. Tests in vacuum show no effect on fatigue life of frequency, a resistance to high temperature fatigue similar to that in air at room temperature, and transgranular cracking at all frequencies.

Specific measurements of crack growth rates in vacuum have also been made [7], and show, in the same austenitic stainless steel, a strong increase in growth rate at frequencies below 10^{-3}Hz. A model has therefore been proposed (Figure 1) schematically comparing crack growth behaviour as a function of frequency in air and vacuum. The diagram shows at high frequencies a frequency-independent transgranular crack growth rate and at low frequencies a purely time-dependent intergranular crack growth rate with a gradient of minus one in the double-logarithmic plot. In a vacuum of 10^{-8}Torr, intergranular creep crack growth is observed at frequencies below 10^{-4}Hz. In air creep crack growth rates are nearly a hundred times more rapid. Fatigue crack growth in air shows an extended transition region between time dependent cracking (below 10^{-3}Hz) and cycle dependent cracking (above 10 Hz). In this range there is a weak dependence on frequency which can be attributed to the interaction of the environment and the unoxidised metal exposed during propagation. In vacuum this environmental influence is removed but the pure time-dependent process becomes important at low frequencies. At intermediate frequencies a super-position model [8] of time and cycle dependent cracking is applicable.

* Brown Boveri Research Centre, 5401 Baden, Switzerland

Vacuum testing may need to be continued down to frequencies $\sim 10^{-4}$Hz to establish whether a frequency effect is present. It was considered of interest to determine the frequency dependence of the crack growth rate in a wrought alloy (Nimonic 105) of moderate creep and oxidation resistance and a cast alloy (IN 738 LC) of high creep and oxidation resistance. The latter alloy is of particular interest because crack branching can occur under certain conditions hence drastically reducing propagation rates [9].

EXPERIMENTAL PROCEDURE

The chemical compositions and heat treatments of the test materials Nimonic 105 and IN 738 LC are given in Table 1. After heat treatment, the former consists of regular grains of diameter ~ 100 µm with carbide particles at the grain boundaries whereas IN 738 LC consists of large irregular grains (~ 3 mm in diameter) containing a dendritic structure with large carbide particles and undissolved γ/γ' eutectic nodules.

Specimens of the alloy Nimonic 105 were of the conventional double cantilever beam type (DCB), and stress intensity amplitudes (ΔK) were calculated from the published formula [10]. However fatigue cracks in cast materials are prone to branching and deviation from the specimen centre line so face grooves were machined in the test blanks, and stress intensity amplitude values were calculated using an experimentally-derived compliance formula [9].

Fatigue testing was carried out on a hydraulic closed-loop machine of ± 10 tons capacity. All tests were performed under load control with sinusoidal waveform and at frequencies in the range 10^2 to 10^{-4}Hz, specimens having been precracked at room temperature and ΔK values lower than in the elevated temperature test. Crack growth rates were determined using the DC potential-drop method, as previously described [9], with an accuracy of better than ± 5%. For elevated temperature tests the specimen temperature in the region of crack growth was controlled to ± 2°C. Air tests were carried out at various ΔK levels whereas tests in vacuum were restricted to the higher values of ΔK, such as to give higher growth rates enabling tests to be continued down to the lowest frequencies.

The chamber used in the vacuum tests is shown schematically in Figure 2. A vacuum of $\sim 2 \times 10^{-6}$ Torr was maintained by the use of heat shields which getter the environment, nickel plating and water cooling of the chamber and "O" ring seals, and slow heating of the specimen to the test temperature. Mechanical loading of the specimen was achieved through movement of the lower arm which was attached to the chamber through a flexible bellows. Specimen heating was by infrared radiation adjusted by a variable transformer. Crack lengths were again determined by the electrical potential-drop technique and crack propagation paths were examined optically on polished sections.

RESULTS

The effect of frequency of fatigue loading on the growth rate of cracks in air and vacuum is shown in Figure 3 for IN 738 LC at 850°C and in Figure 4 for Nimonic 105 at 750°C. At the lower frequencies a definite acceleration in the propagation rate is observed but the effect in air is much smaller in the cast than in the wrought alloy.

Examination of the optical micrographs shown in Figure 5 indicates that, for IN 738 LC at 850°C, as the testing frequency is reduced from 1 Hz to 10^{-4}Hz the crack propagation path in air changes from trans- to intercrystalline and the extent of interdendritic crack branching increases markedly. Heavy oxidation of regions ahead of the crack tips is apparent.

Examination of specimens of Nimonic 105 shows that the increase in growth rate is again associated with a change from mainly transgranular to mainly intergranular propagation, but the alloy is rather less prone to crack branching than is IN 738 LC.

In IN 738 LC propagation rates are not significantly different in air and vacuum at frequencies above 0.1 Hz but below this value growth rates increase rather more rapidly in vacuum than in air. Whereas specimens tested in air show considerable interdendritic crack branching at 10^{-4}Hz (Figure 5b), in vacuum-tested material a single interdendritic crack is still observed (Figure 6). For the wrought alloy growth rates in vacuum deviate below those in air particularly at the lower frequencies.

DISCUSSION

The crack growth results show that Nimonic 105 behaves in a manner consistent with the model of Solomon and Coffin [7] even though in the present study load control and deeply notched specimens were used with pulsating tensile stresses (Push-pull strain-controlled round specimens were used previously [7]). Alloy IN 738 LC shows qualitatively similar behaviour only in vacuum when a single crack can propagate. In air tests crack branching occurs probably due to oxidation and embrittlement of interdendritic regions. These regions are weakened by diffusion of oxygen and the flux of vacancies produced by thickening of the surface oxide may promote cavity formation [11]. The presence of branched cracks in the air tests causes a reduction in ΔK at the crack tip and hence a reduction in propagation rate [12].

To ensure that there was no effect of environment in the vacuum tests the time for the crack to grow one interatomic distance is equated to that required for the formation of an oxygen monolayer on the fresh metal surface [13]. An estimate of the required minimum vacuum pressure of O_2 of 2×10^{-4} Torr is obtained. The actual value achieved was five hundred times lower so that it is believed that there could be no effect of oxidation.

Creep cracking rates are generally observed for wrought alloys to be higher in air than in vacuum [11, 14] but observations of lower growth rates in air have been reported for creep cracking of coarse-grained cast Udimet 700 [15] (though finer-grained material shows the opposite effect) and for creep [16] and fatigue [17] of single crystals of Mar M200. It would be interesting to know to what extent these observations might be understood in terms of crack branching in air tests.

In conclusion, the present data is consistent with the model of Solomon and Coffin [7] for a material which is not prone to crack branching. However for an alloy such as IN 738 LC branching causes the growth rates in air to be reduced below those in vacuum (Figure 7). An implication of the higher growth rate in vacuum for the cast alloy is that at low loading frequencies internal component defects may grow somewhat faster than those intersecting the surface and faster than predicted from laboratory air tests.

ACKNOWLEDGEMENTS

The author would like to thank Dr. M. O. Speidel for useful discussions during the course of this work and Mr. H. Baldinger and Mr. C. Rey for skilled technical assistance.

This work was financed in part by the Swiss Federal Government and performed within the framework of COST-action 50.

REFERENCES

1. ORGAN, F. E. and GELL, M., Met. Trans., 2, 1971, 943.
2. OHMURA, T., PELLOUX, R. M. and GRANT, N. J., Eng. Frac. Mech., 5, 1973, 909.
3. JAMES, L. A., "Stress Analysis and Growth of Cracks", ASTM STP 513, Philadelphia, 1971, 218.
4. SOLOMON, H. D., Met. Trans., 4, 1973, 341.
5. COFFIN, L. F., Jr., Met. Trans., 3, 1972, 1777.
6. COFFIN, L. F., Jr., "Corrosion Fatigue: Chemistry, Mechanics and Microstructure", NACE-2, 590-600, 1972.
7. SOLOMON, H. D. and COFFIN, L. F., Jr., "Fatigue at Elevated Temperatures", ASTM STP 520, Philadelphia, 1972, 112.
8. GALLAGHER, J. P. and WEI, R. P., "Crack Propagation Behaviour in Steels", Int. Conf. on Corrosion Fatigue, June, 1971.
9. SCARLIN, R. B., Mat. Sci. Eng., 21, 1975, 139.
10. SMITH, M. R. and PIPER, D. E., in Stress Corrosion Cracking in High Strength Steels, B. F. Brown, Editor, Naval Research Lab., Washington.
11. LE MAY, I., TRUSS, K. J. and SETHI, P. S., J. Basic Engineering, 91, 1969, 575.
12. SPEIDEL, M. O., "The Theory of Stress Corrosion Cracking in Alloys", NATO Sci. Affairs Div., Brussels, 1971.
13. ACHTER, M. R., Scripta Met., 2, 1968, 525.
14. SKELTON, R. P., Mater. Sci. Eng., 19, 1975, 193.
15. CHAKU, P. N. and McMAHON, C. J., Jr., Met. Trans., 5, 1974, 441.
16. DUQUETTE, D. J., Scripta Met., 4, 1970, 633.
17. DUQUETTE, D. J. and GELL, M., Met. Trans., 3, 1972, 1899.

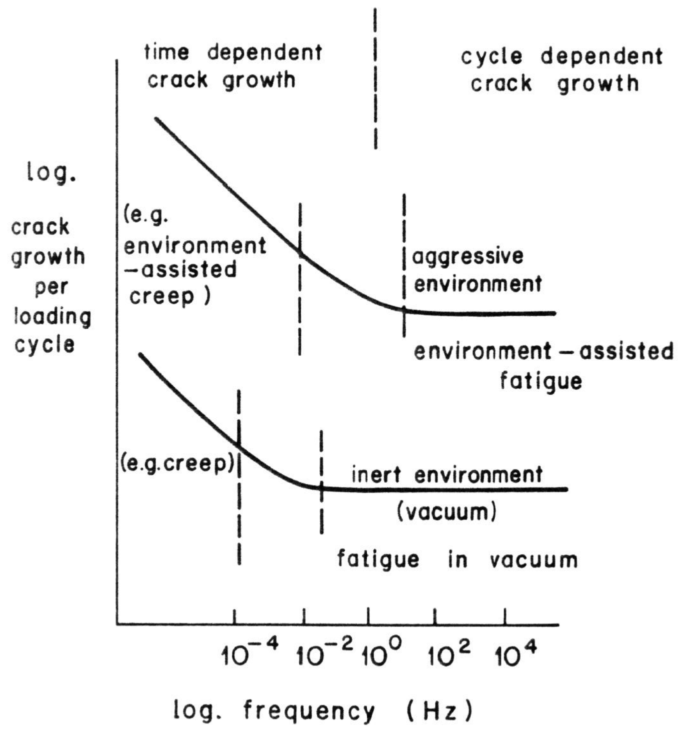

Figure 1 Schematic Comparison of Air and Vacuum Crack Growth Behaviour [7]

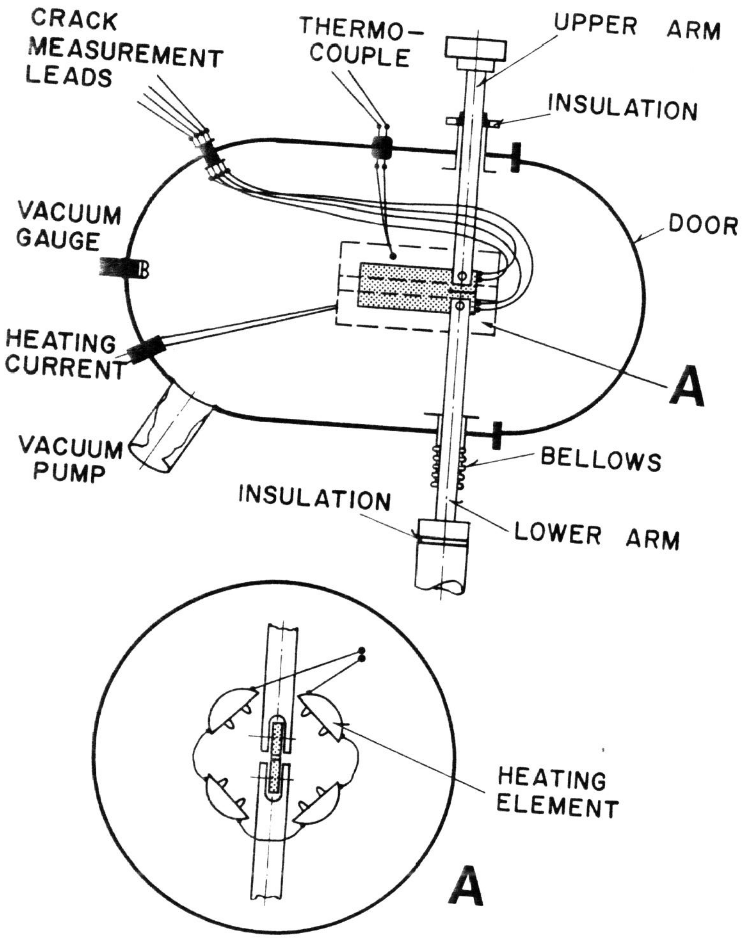

Figure 2 Schematic Diagram of the Vacuum Testing Equipment

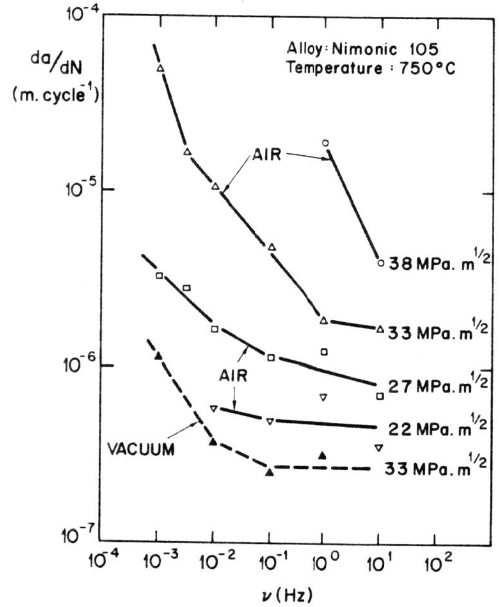

Figure 3 The Dependence of Fatigue Crack Growth Rates in Nimonic 105 at 750° C on Loading Frequency

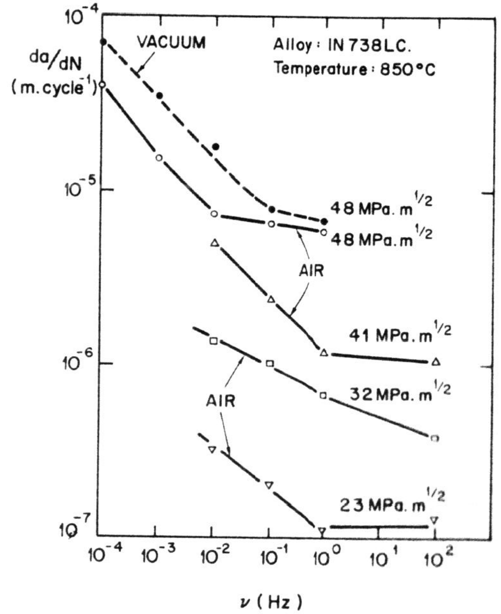

Figure 4 The Dependence of Fatigue Crack Growth Rates in IN 738 LC at 850° C on Loading Frequency

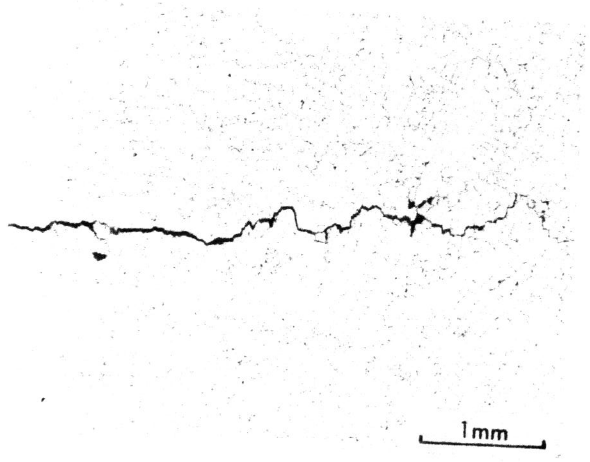

(a)

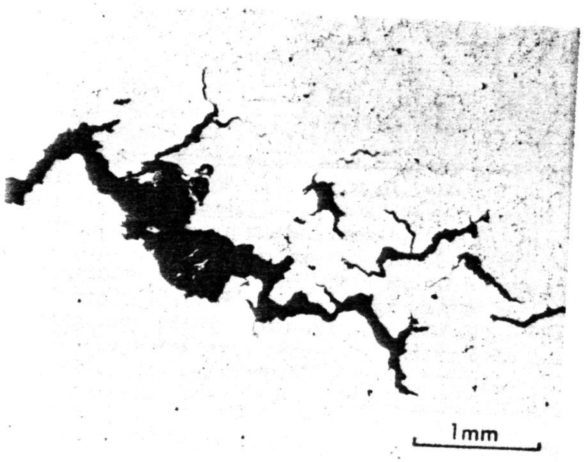

(b)

Figure 5 Optical Micrograph of Cracking in IN 738 LC at 850° C (a) at 1 Hz and (b) at 10^{-4} Hz

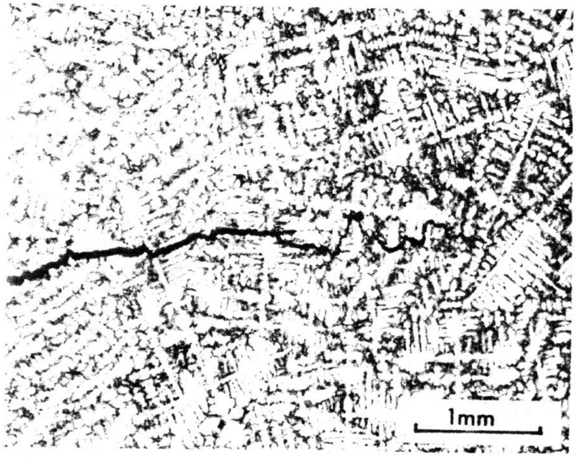

Figure 6 Optical Micrograph of Cracking in IN 738 LC at 850° C in a Vacuum of 2 x 10^{-6} Torr and at 10^{-4} Hz

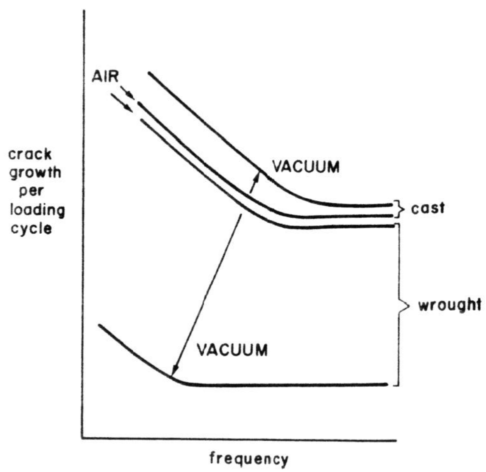

Figure 7 Schematic Representation of the Effect of Environment on Fatigue Crack Propagation in a Wrought and a Cast Nickel-Base Alloy

Table 1 Alloy Compositions and Heat Treatments

Alloy	C	Cr	Co	Mo	W	Ta	Nb	Al	Ti	B	Zr	Heat Treatment
Nimonic 105	0.2	14.5	20.0	5.0	-	-	-	1.2	4.5	-	-	4h/1150°C/AC+ 16h/1050°C/AC+ 16h/850°C/AC
IN 738 LC	0.17	16.0	8.5	1.7	2.6	1.7	0.9	3.4	3.4	0.01	0.10	2h/1120°C/AC+ 24h/845°C/AC